Facies (2017) 63:11
DOI 10.1007/s10347-016-0489-1

ORIGINAL PAPER

Facies variability in mixed carbonate–siliciclastic platform slopes (Miocene)

Jesús Reolid[1] · Christian Betzler[1] · Victoria Singler[1] · Christiane Stange[1] · Sebastian Lindhorst[1]

Received: 1 August 2016 / Accepted: 29 December 2016 / Published online: 25 January 2017

Abstract Miocene tropical carbonate platform slopes in southern Spain contain classical reef-slope facies distribution but also an unexpected abundance of serpulid-rich facies, locally forming build-ups. Two sections from the Miocene Sorbas and Níjar Basins were mapped and analyzed petrographically in order to identify the factors determining this facies variability. Reef-slope facies is intercalated with serpulid-rich facies and siliciclastic bodies. Serpulids are the pioneers colonizing the substrate in zones of quiet hydrodynamic conditions after hydrographical changes such as eventual river discharge. The interplay of sea-level changes and hydrographical conditions, together with episodic terrestrial influx, control lateral and along-slope facies variability as well as the facies distribution across the carbonate platform. Neither a deterministic distribution of facies belts nor a stochastic partitioning of facies in mosaics can accurately explain the facies distribution. A new model is proposed to explain facies variability in the context of intrinsic and extrinsic factors.

Keywords Build-ups · Serpulids · Facies belts · Facies mosaics · Encrusters · Reef

Introduction

Carbonate platform slope facies typically exhibit a zonation into depth-dependent facies belts (Wilson 1975; McIlreath and James 1978; Schlager 2005). The belts are the product of a combination of several intrinsic factors including the initial bathymetry as well as biological and sedimentary processes (Wright and Burgess 2005). This facies belt model alone, however, cannot explain the complex facies variability observed in carbonate slope outcrops. Calcium carbonate production areas may arise in patchworks or mosaics and along-slope processes may be localized (Wright and Burgess 2005). Many of these mosaic elements are not depth-dependent and can change through time due to the influence of subtle extrinsic factors, i.e. siliciclastic input in the carbonate factory (Wright and Burgess 2005).

Miocene tropical carbonate platform slopes crop out in the Neogene basins of the Betic Cordillera in southeast Spain and were the subject of numerous studies (Esteban 1980; Dabrio et al. 1981, 1985; Riding et al. 1991; Martín and Braga 1994; Braga and Martín 1996; Esteban 1996; Franseen and Goldstein 1996; Cuevas-Castell et al. 2007). In cross section, both the Cariatiz carbonate platform in the Sorbas Basin and the Polopos carbonate platform in the Níjar Basin display a progradational pattern with well-developed clinoform bodies. These clinoform bodies have a downslope facies zonation, from reef-framework blocks and breccia to fine-grained packstone. This facies zonation may change in distinct growth packages depending on available accommodation space ultimately related to sea-level fluctuations (Reolid et al. 2014).

Slope facies and microfacies distribution exhibit a high degree of variability, which is mainly due to the presence of abundant serpulids and siliciclastics. This study addresses the causes and significance of the factors determining this facies distribution in carbonate platform slope clinoform bodies. We discuss how it is a consequence of exposure to water turbulence and hydrographic perturbations in response to phases of enhanced continental runoff.

✉ Jesús Reolid
jesus.reolid@uni-hamburg.de

[1] Institut für Geologie, Universität Hamburg, Bundesstraße 55, 20146 Hamburg, Germany

Geological setting

Carbonate platform slopes crop out in the intramontane Neogene basins of southeast Spain (Fig. 1). Two sections from the Cariatiz carbonate platform, the Barranco de la Mora and Barranco de los Castaños sections, at the northern margin of the Sorbas Basin, and two sections from the Polopos and Níjar carbonate platforms at the northern margin of the Níjar Basin were analyzed (Fig. 1). The Sierra de los Filabres with metamorphic rocks from the Internal Betic Zone borders the E–W-elongated Sorbas Basin to the north, the Sierra Alhamilla and Sierra Cabrera bound it to the south (Fig. 1). There, a Messinian carbonate platform with coral reefs (Fringing Reef Unit, Riding et al. 1991; Braga and Martín 1996) and related basinal silty marls, marls and diatomites from the Upper Abad Member (Martín and Braga 1994) is cut by several ravines, which provide insights into the platform-internal and slope-facies architecture (Fig. 2a). The Sierra Alhamilla and Sierra Cabrera border the NE–SW elongated Níjar Basin to the north, the Neogene volcanic complex Cabo de Gata bounds it to the southeast. A Messinian carbonate platform with coral reefs and associated basinal silty marls from the Upper Abad Member occurs at the northern margin of the basin (Fig. 2b; Dabrio et al. 1981).

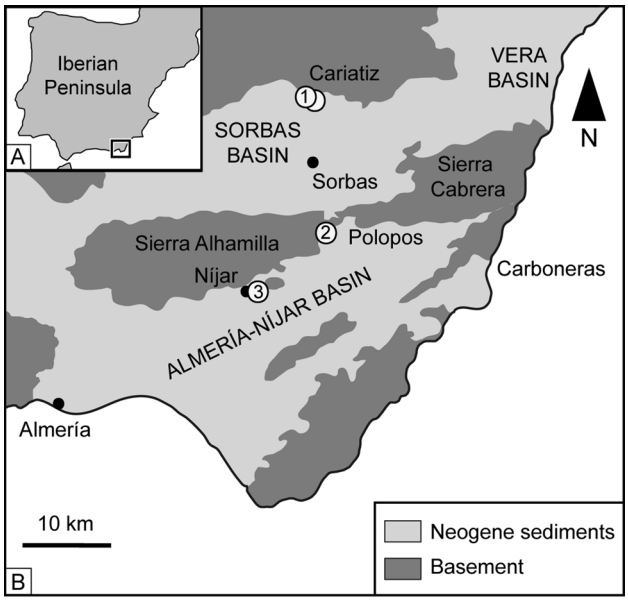

Fig. 1 *A* Location map of the study area in SE Spain. *B* Regional setting of the Neogene basins of SE Spain showing the carbonate platform discussed in this study: Cariatiz (Barranco de la Mora and Barranco de los Castaños sections), Polopos and Níjar

Methods

Carbonate platform slope facies were mapped using panoramic photomosaics of the best-exposed successions. Two hundred samples from different facies were petrographically analyzed to identify microfacies and components. In addition, polished slabs were used to analyze large bioclasts, sedimentary fabrics, and structures. Where possible, the slopes of the Cariatiz carbonate platform were scanned with an Optech Laser Imaging ILRIS 3D terrestrial LIDAR. The LIDAR data were digitally processed using 3D-Reconstructor (Gexcel). Slope dimensions and slope angles in the Barranco de los Castaños section were previously presented by Reolid et al. (2014).

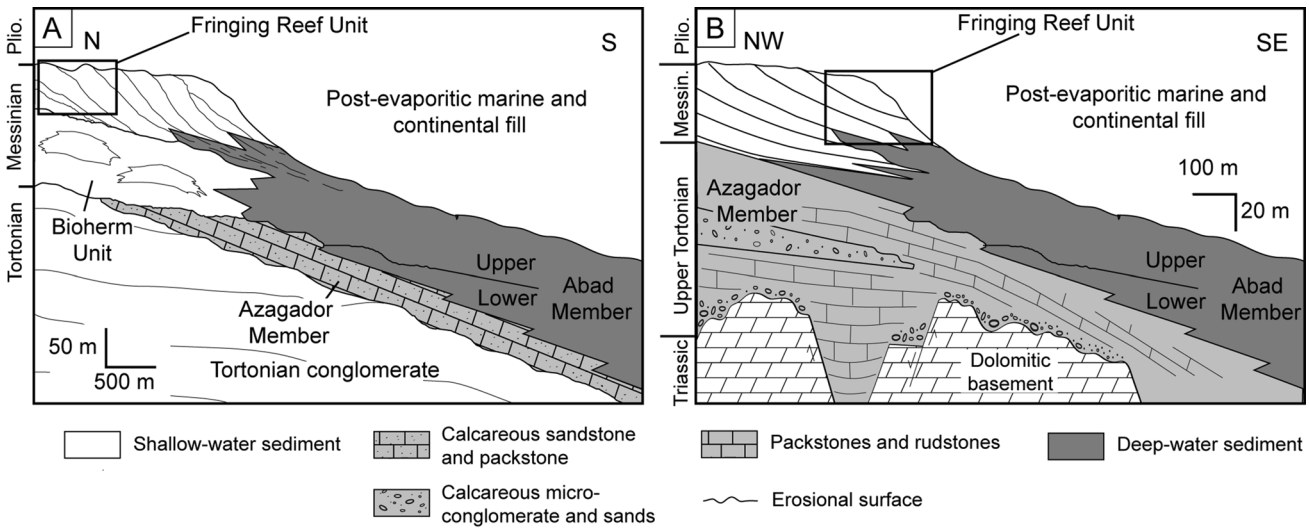

Fig. 2 **a** Neogene lithostratigraphy of the Sorbas Basin. The *rectangle* indicates the interval of the succession shown in detail in Fig. 3 (Modified from Reolid et al. (2014)). **b** Neogene lithostratigraphy of the Polopos area. The *rectangle* indicates the interval of the succession shown in detail in Fig. 7

Table 1 Platform-slope facies of Barranco de la Mora section

Facies	Components	Matrix	Fabric	Coatings	Position	Dip
Breccia	5–300-cm reef-framework blocks Coralline algae, bivalves, gastropods, echinoid spines, bryozoans, serpulids, benthic foraminifera (mainly miliolids), and rare *Halimeda* plates Intraclasts and siliciclastics (quartz and mica)	Microgranular matrix (wackestone-packstone of unidentifiable bioclasts)	Chaotic Massive	Red algae (especially on serpulids and bivalves)	Talus slope	35°–25°
Bioclastic floatstone	Up to 4-cm-large bioclasts including echinoid spines, bivalve fragments, benthic foraminifera (usually miliolids), and red algae, and minor coral fragments, gastropods, serpulids, and bryozoans Locally 3–11-mm *Halimeda* plates rudstones (up to 80% of the rock) Siliciclastics (quartz and mica)	Microgranular matrix (wackestone of silt-sized bioclasts)	30–70-cm beds Shells are locally in contact in grain supported patches with similar proportions of concave- and convex-up orientation 60–100-cm-thick and 3–4-m-wide *Halimeda* mound	Red algal coatings	Proximal slope	25°–15°
Bioclastic wackestone to floatstone	Bivalves (Pectinidae, Glycymerididae, Veneridae, Mytilidae, and Ostreidae), solitary corals, bryozoans, red algae, benthic and planktonic foraminifera, and minor serpulids and *Halimeda* plates Siliciclastic up to 15% of the facies	Marls	30–40-cm-thick beds Shells are randomly oriented to bedding with similar proportions of convex- and concave-up orientation	Serpulids, bryozoans, and red algae	Distal slope	15°–10°
Serpulid boundstone	Clusters and up to 2-mm fragments of serpulids (about the 85–90% of the rock) Bryozoans, red algae, and oysters Siliciclastic grains (up to 10%), mostly phylosilicates, and scarce intraclasts	Microgranular matrix (wackestone-packstone of silt-sized bioclasts)	Patches of articulated oysters in life position	Serpulids, bryozoans, and red algae	Talus to proximal slope	30°–20°
Serpulid-red algal rudstone to floatstone	Up to 20-cm serpulid-red algal nodules Bryozoans, bivalves, gastropods, echinoids, and rarely coral fragments Intraclasts	Marls, locally microgranular carbonate matrix	10–30-cm-thick beds Locally parallel lamination and subparalel orientation of bivalves Alternance of thin limes and marls beds and thick nodule-accumulation beds	Serpulids, bryozoans, and red algae	Distal slope	20°–5°

Table 1 continued

Facies	Components	Matrix	Fabric	Coatings	Position	Dip
Bioclastic packstone-rudstone (lowstand wedges)	Up to 4-cm red algal nodules Bryozoans, serpulids, bivalves, echinoid spines, and benthic foraminifera	Microgranular matrix	30–60-cm-thick thinning-upward beds	Red algae and bryozoans	Proximal to distal slope	30°–15°
Siliciclastics	Up to 10-cm quartz, schist, marble and serpentinite clasts Serpulids, benthic foraminifera, echinoid spines, bryozoans, and red algae	Mixture of sand and microgranular carbonate matrix	Poorly bedded	Bryozoans, serpulids, and red algae	Talus to distal slope	30°–15°

Results

Carbonate slope facies

The characteristics of the main slope facies of the Messinian fringing reef-slopes are summarized in Tables 1 and 2. Locally, there are facies containing up to 50% siliciclastics (Tables 1, 2). Individual slope bedsets may consist entirely of siliciclastics.

Barranco de la Mora section: slope facies distribution

The more than 190-m-long Barranco de la Mora section in the northwestern part of the Cariatiz carbonate platform contains several carbonate platform growth packages (Fig. 3). The slope facies, described in Table 1, occur in 14 sedimentary bodies, including reefal clinoform bodies (CB), serpulid build-ups, lowstand wedges, and siliciclastic-rich bodies (Fig. 3).

Clinoform bodies

In the Barranco de la Mora section, there are seven clinoform bodies. The maximum thickness of these bodies is 7 m, and the maximum extension in the direction of progradation (~N170E) is 80 m. The slope angles vary from up to 35° at the reef talus to 25° at the proximal slope, and 15° at the distal slope. The facies distribution follows the model presented by Riding et al. (1991). The uppermost facies in these clinoform bodies is the breccia facies (Fig. 4a), with an average thickness of 5 m. *Porites* sticks corals can be found in the reef-framework blocks. Reef-framework debris size and amount decrease basinward and the lithology gradually changes into a bioclastic floatstone in the proximal slope.

In the proximal reef-slope, a 60–100-cm-thick and 3–4-m-wide mound consisting of an accumulation of *Halimeda* plates occurs within one of the clinoform bodies (CB3 in Fig. 3). The *Halimeda* plates range in size from 2 to 10 mm in section and make up a rudstone with minor micritic matrix in the remaining pore spaces (Fig. 4b).

The gradual transition from the proximal to the distal slope deposits corresponds to a well-bedded bioclastic wackestone to floatstone facies fining downslope (Fig. 4c). Where present, bioturbation is confined to the finest intervals. Some beds host patches rich in bivalves, mainly from the families Veneridae, Glycymeridae, and Pectinidae.

Serpulid build-ups

These bodies are up to 6 m thick and are up to 70 m wide in slope normal direction. Their uppermost part consists of serpulid boundstone (Fig. 5a, b), while there is a downslope change towards accumulations of serpulid debris (Fig. 5c, d). The serpulid-rich bodies are faintly bedded. Bedding is better-developed downslope, where other bioclasts, especially red algae and bivalves, are common. In these areas, the deposits are marls.

Clinoform body 5 (Fig. 3) contains a mixture of serpulid build-up and reef-related facies including a breccia with large reef-framework blocks to the top. The proximal slope is covered by vegetation and it is not possible to identify the facies. The distal slope consists of an accumulation of serpulid-red algal nodules arranged in 20–30-cm-thick beds locally deformed by the load and dredging effect of large reef-framework blocks. The nodules range in size from 5 to 20 cm and consist of clusters of red algae, serpulids, and minor bryozoans (Fig. 5e). An alternation between thin fine-grained beds and thick nodule-accumulation beds occurs (Fig. 5f). The fine-grained beds

Table 2 Platform-slope facies of Polopos section

Facies	Components	Matrix	Fabric	Coatings	Position	Dip
Siliciclastic-coral breccia	Fragments of reef-framework debris (cm to m scale), red algae, bryozoans, serpulids, bivalves, benthic foraminifera, echinoid spines, and solitary corals Siliciclastics (pebble to cobble-size) between to 25–30% (locally up to 50%)	Microgranular to dense/clotted/peloidal micrite	Chaotic Locally centimetric to decimetric siliciclastic beds	Red algae and locally stromatolites	Talus slope	35°–20°
Halimeda breccia	*Halimeda* plates, framework blocks (m to cm), gastropods, bivalves, red algae (locally as rhodoliths), foraminifera, fragments of solitary corals, bryozoans, echinoid spines, serpulids, and barnacles Sand to pebble siliciclastic content up to 7%	Dense micrite (locally microgranular)	Massive to poorly bedded Locally patches formed by red algal crusts and serpulid tubes among a microbial to micritic matrix	Red algae, serpulids, and barnacles	Talus slope	25°–20°
Siliciclastic-coral floatstone	Up to 2 cm fragments of corals, bivalves, red algae, bryozoans, gastropods, echinoid spines, and miliolids Sand to pebble siliciclastic content up to 10%	Silt- to sand-sized siliciclastic grains in a micritic matrix	Massive to poorly bedded	Red algae	Proximal slope	20°–15°
Siliciclastic-red algal-serpulid rudstone	Sand to pebble sized fragments of serpulids, red algae, bivalves, bryozoans, miliolids, gastropods, and echinoid spines Up to 15-cm siliciclastics between 5 and 15% of the facies	Microgranular (rarely micritic)	Alternating bedding of centimetric to decimetric rudstone and floatstone beds	Serpulids and red algae (preferentially on large siliciclastics). Bryozoans	Proximal slope	20°–15°
Serpulid rudstone	Up to 2-cm-large bioclasts including serpulids, bivalves, red algae, miliolids, and rarely echinoid spines, bryozoan, gastropods, barnacles, and coral fragments Up to 4-cm-large siliciclastics are the 5% of the facies	Micritic to microgranular	20-cm-thick and 15–40-cm-wide patches of in situ encrustation of serpulids 10–50-cm-thick beds alternating coarser and finer rudstones. Beds with locally wavy bottoms. Decimetric siliciclastic-rich beds intercalated	Serpulids and red algae	Proximal slope	20°–15°

Table 2 continued

Facies	Components	Matrix	Fabric	Coatings	Position	Dip
Red algal-bivalve packstone to floatstone	Sand-sized bioclasts (locally up to 15 cm) including red algae, bivalves (pectinids and oysters), corals, bryozoans, gastropods, serpulids, benthic foraminifera, echinoid spines, and rarely planktonic foraminifera Sand to pebble siliciclastics up to 10%	Micrite	Alternation of 20–100-cm greyish bioturbated floatstone intervals and reddish stratified packstone beds	Micritic envelopes	Proximal to distal slope	15°–10°
Siliciclastic-rich packstone to rudstone	Red algae, bivalves, serpulids, corals, gastropods, echinoid spines, and barnacle fragments The amount of siliciclastics can be up to 35% (up to 5 cm)	Micritic to locally microgranular	Alternation of decimetric packstone and rudstone beds	Red algae	Proximal to distal slope	15°–10°
Siliciclastics	Up to 5-cm quartz, schist, marble, and serpentinite clasts Serpulids, benthic foraminifera, echinoid spines, bryozoans, and red algae	Mixture of sand and microgranular carbonate matrix	Poorly bedded	Bryozoans, serpulids and red algae	Talus to distal slope	25°–15°

consist of marls alternating with sand-grade carbonate bioclasts.

Siliciclastic bodies

Two siliciclastic intervals, each up to 3 m thick, are intercalated into the carbonate platform-slope succession (Fig. 3). The stratigraphically older body (SRB1 in Fig. 3) consists of a conglomerate with up to 5-cm clasts in a sand-sized matrix, which is a mixture of siliciclastic and carbonate grains. Most of the siliciclastic pebbles are encrusted with bryozoans representing the first generation of encrusters followed by serpulids and red algae (Fig. 6). The younger body (SRB2 in Fig. 3) consists of a faintly bedded mixed carbonate-siliciclastic sand with unidentifiable sand-sized bioclasts.

Lowstand wedges

The platform-slope succession contains two packages of well-bedded bioclastic packstone to rudstone, with a maximum thickness of 8 m and an extension of 40 m (Fig. 3). The bodies thin out upslope.

Polopos section: slope facies distribution

A succession of seven SE-prograding clinoform bodies extending over 300 m provides a good overview of the slope facies arrangement of this carbonate platform (Fig. 7). The slope facies, described in Table 2, occur in seven sedimentary bodies, including reefal clinoform bodies (CB) with intercalated siliciclastic bodies.

In their uppermost part, the clinoform bodies comprise the reef-framework facies with *Porites* stick surrounded by thick stromatolithic crusts. The coral colonies form subvertical cliffs with an inclination of 80°–60° (Fig. 8a). The thickness of the reef-framework facies commonly varies from 10 to 15 m with a slope normal extension between 15 and 25 m. The reef-framework facies may contain up to 15% siliciclastics ranging from sand-sized (Fig. 8b) to pebble-sized (Fig. 8c). Locally, lagoonal facies overlies the reef framework (Fig. 7).

The reef-talus slope facies has an inclination of 25° and consist of a *Halimeda* breccia with large reef-framework debris (Fig. 9). *Halimeda* breccia packages are 5–15 m thick and extend between 10 and 70 m in slope normal direction. In the case of CB1 and CB5 (Fig. 7),

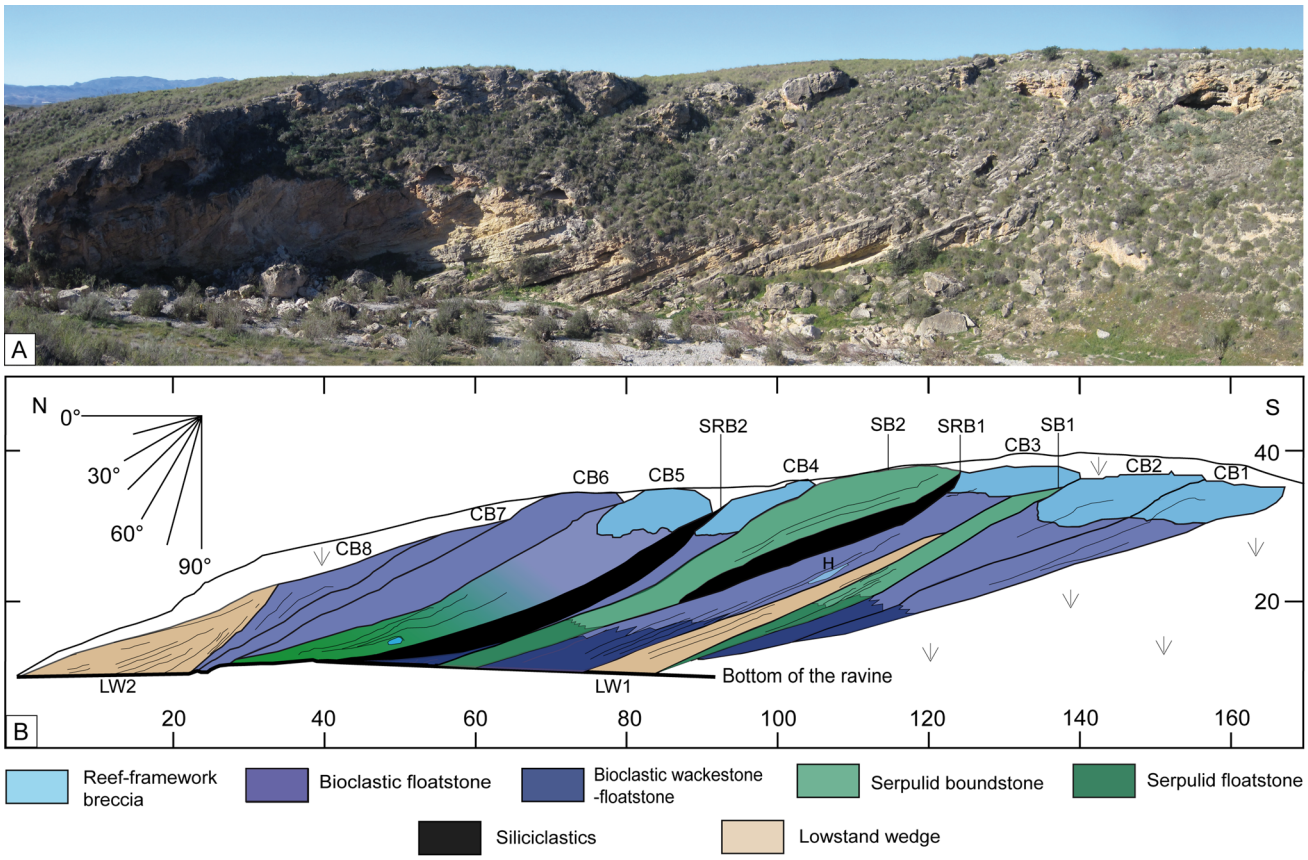

Fig. 3 **a** Outcrop panorama of the Barranco de la Mora section in the Cariatiz carbonate platform. **b** 2D projection of main surfaces derived from a LIDAR data set and traced onto a plane oriented in parallel to the direction of progradation (N170E). The slope facies form 14 sedimentary bodies, including reefal clinoform bodies (CB) with a *Halimeda* mound (H), serpulid build-ups (SB), lowstand wedges (LW), and siliciclastic-rich bodies (SRB)

the talus-slope facies is a siliciclastic-coral breccia with a maximum thickness of 15 and a 70-m extension in slope normal direction. Sandstone to conglomerate beds locally cut across the siliciclastic-coral and the *Halimeda* breccia (Fig. 9).

The proximal Polopos carbonate platform slope display angles of 20°–15° with a considerable facies variability. The facies may consist of (1) a siliciclastic-red algal-serpulid rudstone, locally displaying an alternation of floatstone intervals with rudstone beds (Fig. 10a, b); (2) a serpulid rudstone (CB3 and CB7 in Figs. 7, 10c, d); and (3) a siliciclastic-coral rudstone.

The distal slope has inclinations between 15° and 10° and consists of red algal-bivalve packstone to floatstone that may interfinger with the proximal slope facies in its upper part. The thickness of the red algal-bivalve packstone to floatstone facies decreases downslope from 10 to 5 m. Where the siliciclastic content is high, the red algal-bivalve facies occurs as a siliciclastic-rich packstone to rudstone (CB5 and CB6 in Fig. 7).

In general, the reef-slope facies are rich in siliciclastics. The thickest siliciclastic body is a 2-meter-thick greyish conglomeratic sandstone intercalated between CB2 and CB3 (Figs. 7, 9).

Discussion

Miocene slope facies composition and distribution

The slope-facies composition and distribution result from the interaction of several factors including coral growth, in situ slope carbonate production, rockfalls and sediment gravity flows, hemipelagic rain and reworking of reef-slope facies, as well as siliciclastic input (Reolid et al. 2014). Changes in accommodation space related to sea-level fluctuations shaped the relative impact of these factors (Reolid et al. 2014).

Porites-stromatolite reef framework rims the uppermost part of most of the Miocene tropical carbonate platform slopes in southeastern Spain (Fig. 11). Stromatolites

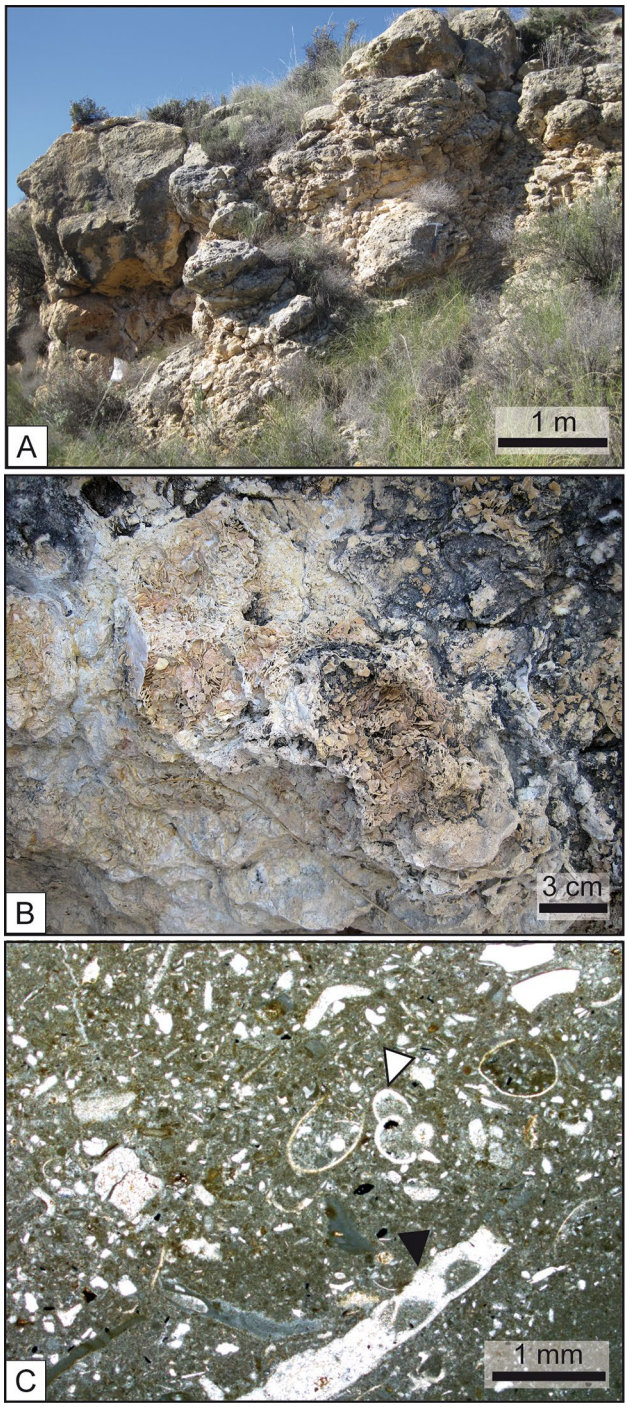

Fig. 4 Clinoform body facies in the Barranco de la Mora section. **a** Breccia facies in the talus slope with large *Porites*-framework blocks. **b** Close-up of the *Halimeda* mound in the proximal slope of CB3 (Fig. 3). **c** Photomicrograph of the distal-slope bioclastic wackestone with bryozoan fragments (*black arrow*) and planktonic foraminifera (*white arrow*) in a silt-sized bioclastic matrix with minor siliciclastics

encrusted the *Porites* colonies, producing an early lithification (Riding et al. 1991). The breakage of the *Porites*-stromatolite framework at the reef front subsequently produced rock and debris falls (Dabrio et al. 1981; Riding et al. 1991). This process resulted in the accumulation of blocks and debris on the reef-talus slope as described for the Barranco de la Mora and the Polopos sections (Figs. 4, 9, 11). Rockfalls and debris falls triggered sediment flows that spread basinward to the distal reef-slope with decreasing transport capacity (Adams et al. 1998; Reolid et al. 2014). Under conditions of low accommodation space, these rockfalls may export large reef-framework blocks to more distal settings than during conditions of high accommodation space, as recorded in the Barranco de los Castaños section (Fig. 11; Reolid et al. 2014). During lowstand periods, the erosion and reworking of the slope deposits intensified, resulting in the accumulation of bioclastic sands in fan-like bodies, which form the lowstand wedges of the Cariatiz carbonate platform (Fig. 11; Braga and Martín 1996; Cuevas-Castell et al. 2007).

Halimeda plates are the main facies component in Miocene carbonate platform slopes of southeastern Spain (Mankiewicz 1988; Martín and Braga 1990; Riding et al. 1991; Braga and Martín 1996; Reolid et al. 2014). *Halimeda* plates either accumulated in situ as small mound-like structures as in Barranco de la Mora section (Fig. 4b) or were exported downslope by sediment flows, forming parautochtonous to allochtonous accumulations along the slope as in the Polopos section (Fig. 10). Mankiewicz (1988) described similar *Halimeda*-rich facies and related them to upwelling conditions. Reolid et al. (2014) proposed that upwelling of nutrient-rich waters during sea-level rise and highstand stages promoted the flourishing of *Halimeda* in the Barranco de los Castaños section. The decreasing accommodation space with continued sea-level fall promoted the mixture of water masses and consequently the interruption of upwelling the absence of *Halimeda* algae (Reolid et al. 2014). Under such conditions, bioclastic packstone to rudstone formed with common bivalves, gastropods, echinoids, red algae, serpulids, and benthic foraminifera as described in the Barranco de los Castaños section (Reolid et al. 2014) and in the Barranco de la Mora and Polopos section (Fig. 11). Turbidity currents by episodic river discharge are an additional factor that may affect the substrate colonization by *Halimeda* algae and their development (Mankiewicz 1988).

Silt and marl in the distal reef-slope (Fig. 11) indicate relatively quiet-water conditions (Sánchez-Almazo et al. 2001, 2007). The extension of distal slope facies may diminish in clinoform bodies deposited during sea-level fall and lowstand (Fig. 11).

Slope facies variations: serpulid build-ups and siliciclastics

The carbonate platform slopes have a higher degree of facies variability in comparison to other Miocene carbonate

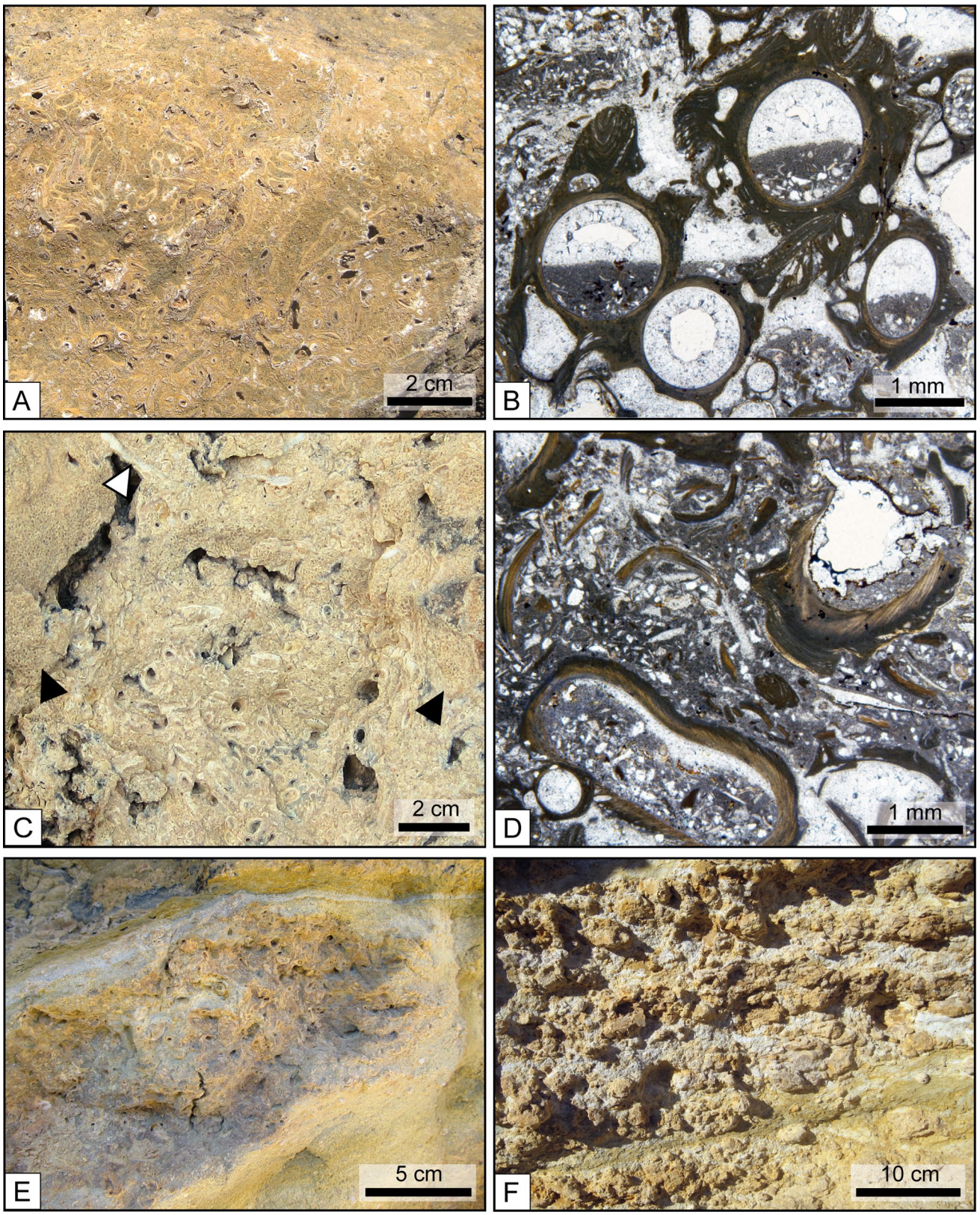

Fig. 5 Serpulid-rich facies in the Barranco de la Mora section. **a** Close-up of the surface of the serpulid boundstone of SB2 (Fig. 3). **b** Photomicrograph of the serpulid boundstone. **c** Close-up of the serpulid rudstone of SB1 with oyster debris (*white arrow*) and abundant bryozoan coatings (*black arrows*). **d** Photomicrograph of the serpulid rudstone with common fragmentation of the serpulid tubes. **e** Close-up of a serpulid-red algal nodule floating in a marl matrix from the distal slope of CB5. **f** Outcrop picture of the distal slope of CB5 with an alternance of thin marl beds and thick nodule-rich beds

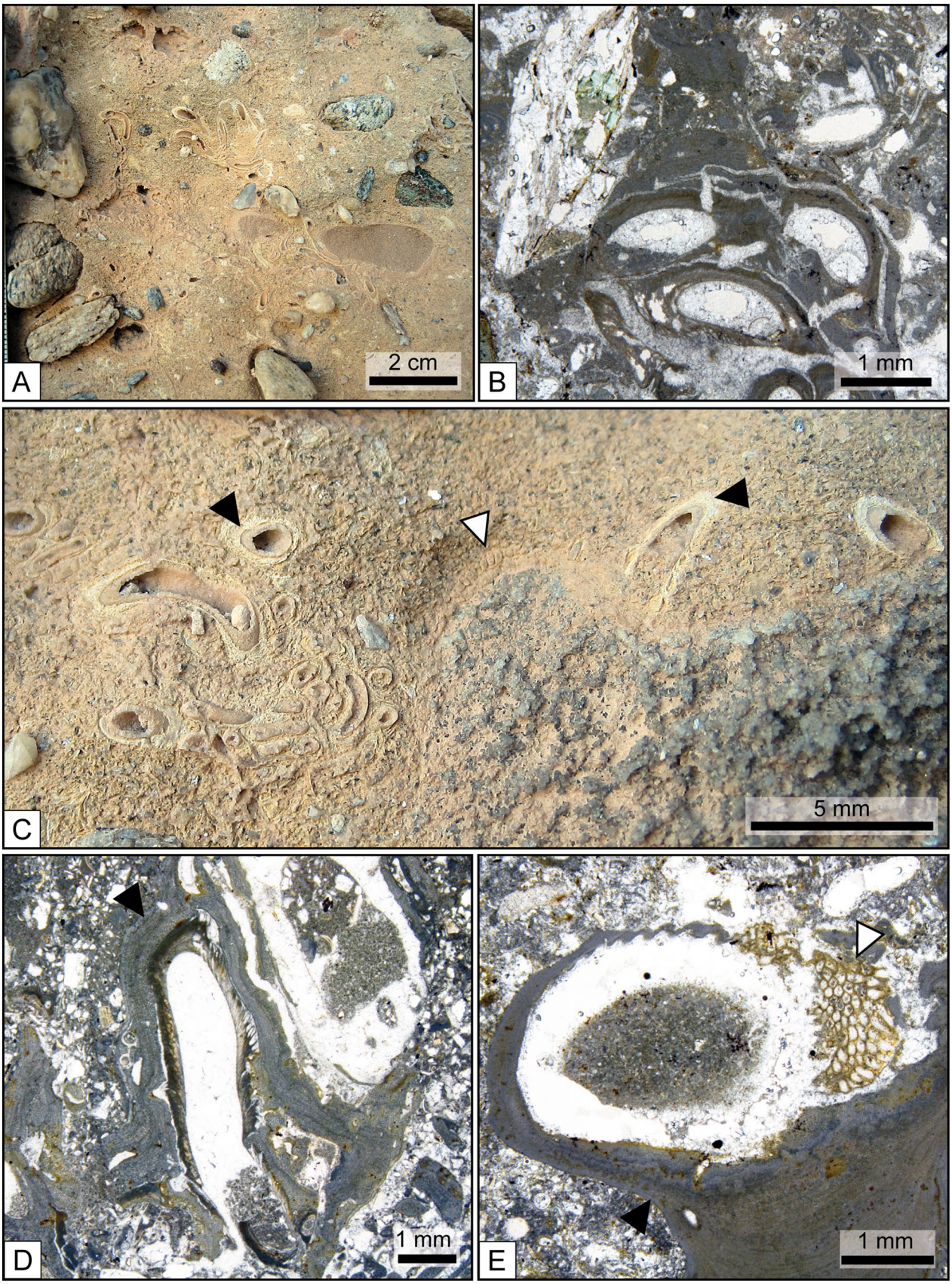
A
2 cm
B
1 mm
C
5 mm
D
1 mm
E
1 mm

◂**Fig. 6** Siliciclastic-rich facies and encrusters of the Barranco de la Mora section. **a** Close-up of the siliciclastic-rich facies with abundant serpulids. **b** Photomicrograph of the siliciclastic-rich facies with serpulids (SRB1, Fig. 3). **c** Close-up of a pebble from the siliciclastic-rich facies encrusted by bryozoans (*white arrow*) and serpulids. Serpulids are encrusted by red algae (*black arrow*). **d** Photomicrograph of a bioclastic floatstone with common siliciclastic and serpulids encrusted by red algae (*black arrow*). **e** Photomicrograph of a bioclastic floatstone with common siliciclastics showing a large bioclast encrusted by bryozoans (*white arrow*) and by red algae (*black arrow*)

platform slopes from southeastern Spain (Fig. 11). This facies variability depends on the intercalation of serpulid-rich and siliciclastic-rich facies in the typical slope sediments.

Facies variability related to siliciclastics

During the Neogene, carbonate platform growth in southeastern Spain was coeval with fan-delta sedimentation (Braga et al. 1990), and therefore these platforms underwent episodic input of coarse-grained sands and conglomerates (Fig. 11; Braga et al. 1996). Siliciclastic shedding in the Sorbas Basin started during the early Messinian, related to the uplift of the Sierra de los Filabres and Sierra Alhamilla (Braga et al. 2003). In the Polopos area, the siliciclastic input was triggered by the synsedimentary tectonic activity of the reverse Polopos fault, which delimits the carbonate platform to the northwest (Pedrera et al. 2012; Giaconia et al. 2012). In addition to the tectonic activity, the intensification of weathering may control the siliciclastic influx, which varied independently of sea-level changes (Braga and Martín 1996).

In the Barranco de la Mora area, two siliciclastic-rich fan delta bodies (Fig. 3; Table 1) contain a conglomerate in the most proximal part (SRB1 in Fig. 3), and sands in the distal part (SRB2 in Fig. 3). In the Polopos area the influence of the continental discharge is greater than in the Barranco de la Mora area with a complete range of siliciclastic-rich facies from pure fan delta deposits (Siliciclastics in Fig. 7; Table 2) to mixed facies where the fan delta mixed with the talus-slope breccia, siliciclastic-coral breccia, or mixed with the different proximal-slope facies, such as siliciclastic-coral floatstone, siliciclastic-red algal-serpulid rudstone, and siliciclastic-rich packstone to rudstone (Fig. 7; Table 2).

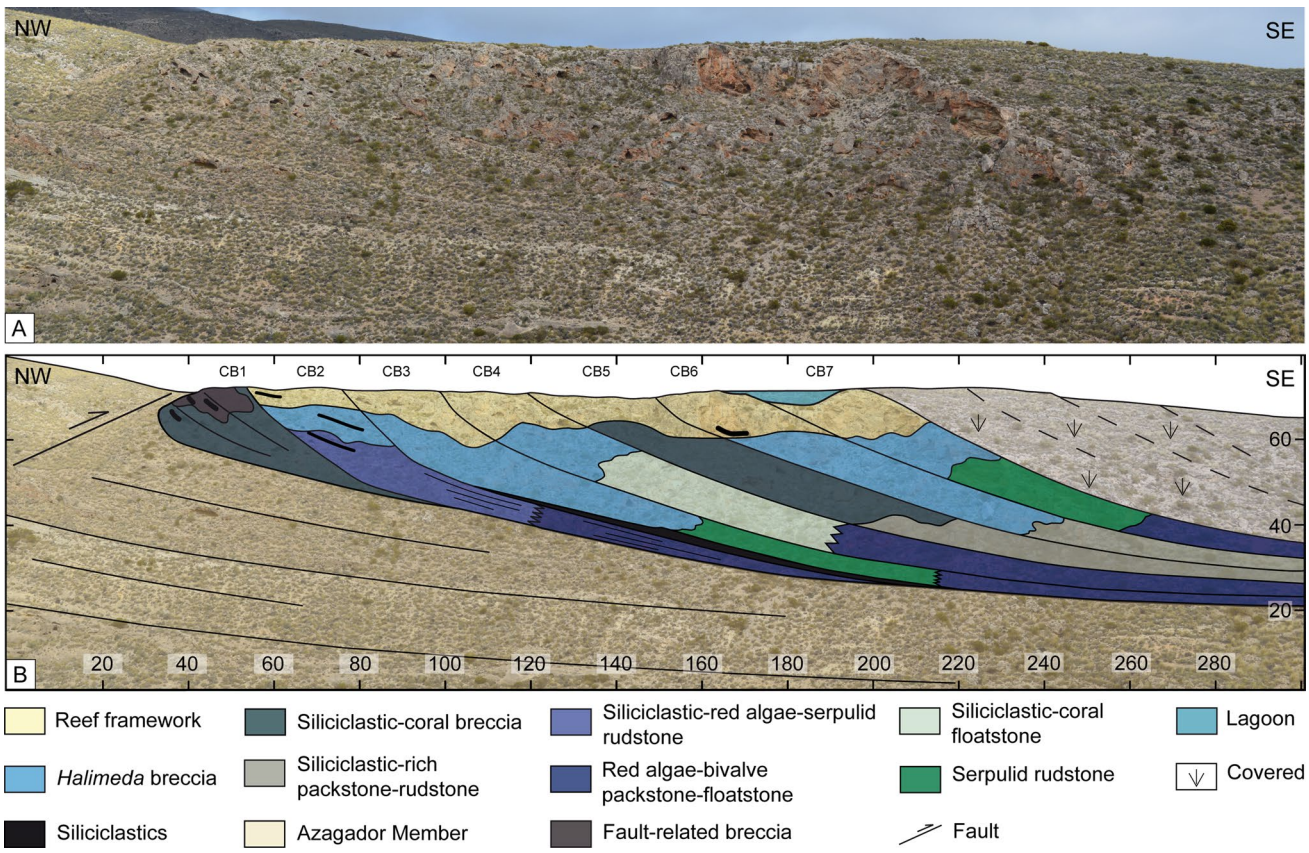

Fig. 7 **a** Outcrop panorama of the Polopos section. **b** Interpretation of the main clinoform bodies (CB), bedding, and facies

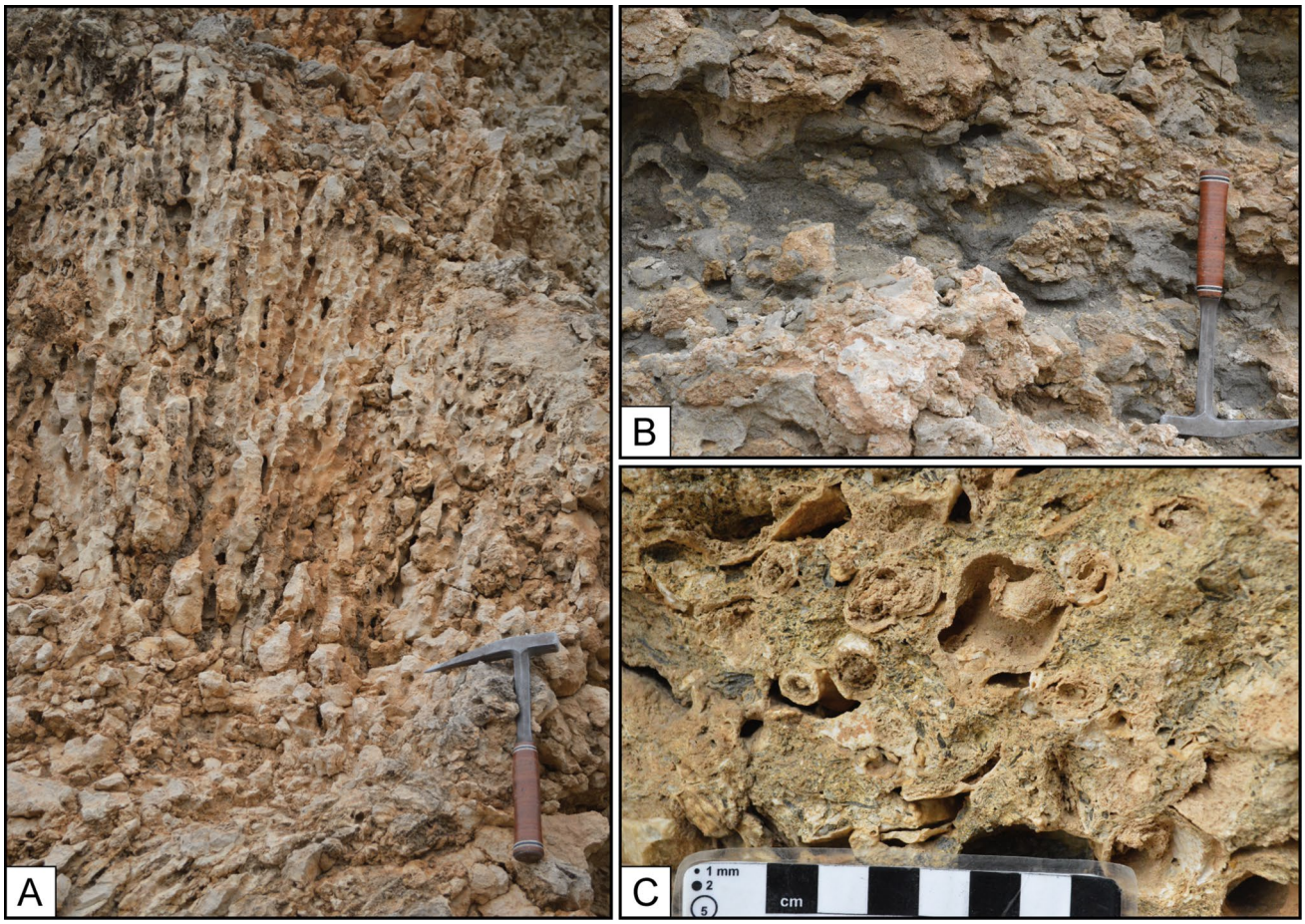

Fig. 8 **a** Outcrop picture of the reef-framework facies with *vertical Porites* tubes and thick stromatolitic crusts from CB3 (Fig. 7). **b** Outcrop example of fine grained siliciclastics in the gaps among stromatolitic crusts at the base of the reef framework. **c** Outcrop example of coarse siliciclastic grains among *horizontal Porites* tubes in the transition from the reef framework to the siliciclastic-coral breccia

Facies variability related to build-ups

Large serpulid build-ups, comparable to those from the Barranco de la Mora section, require low-energy settings which allow larval settlement (ten Howe and van den Hurk 1993; Qian 1999). Modern serpulid build-ups occur exclusively in low-energy settings such as Albufera of Menorca, in the Balearic Islands (Fornós et al. 1997) and the Galway Bay in Ireland (Bosence 1973). The area of the Barranco de la Mora section was probably a quiet environment with marls and limestones deposited in calm waters of the shallow distal slope (Sánchez-Almazo et al. 2001, 2007) between 30 and 40 m (Fig. 3). A low-energy environment is congruent with the restricted occurrence of the *Halimeda* plates in CB3 that remained mostly in situ and were rarely transported downslope in contrast to other carbonate slopes in the area (Fig. 11; Reolid et al. 2014). The patches of bivalves in the distal slope deposits represent allochthonous assemblages, eventually exported downslope from the proximal slope as is the case in the Níjar platform slope (Jiménez and Braga 1993). Occasional events of increased hydrodynamic energy, however, in this part of the carbonate platform is indicated by the presence of centimetre-sized terrigenous clasts.

The average hydrodynamic energy at the distal slope with packstones to rudstones was higher in the area of Polopos. The siliciclastic input in Polopos was also more significant with frequent terrigenous clasts throughout the section. Such conditions may explain why serpulids, although abundant in the Polopos slopes did not form build-ups there but patches similar to those described in other Messinian carbonate platform slopes (Sola et al. 2013; Reolid et al. 2014).

Salinity appears as another factor controlling serpulid buildup. In Menorca, low salinity apparently favors

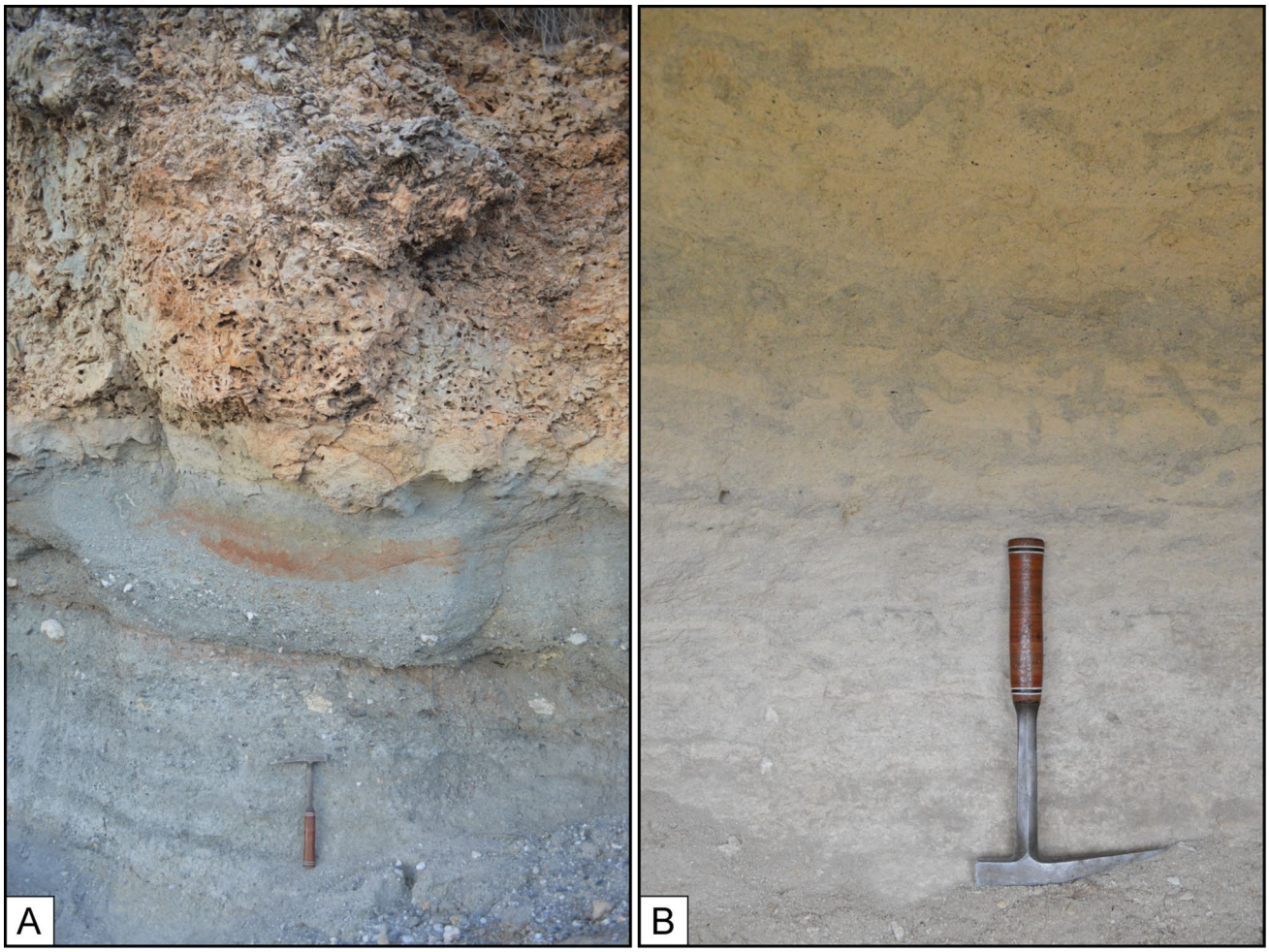

Fig. 9 **a** Outcrop picture of large framework blocks from the *Halimeda* breccia facies of CB3 overlying a thick siliciclastic body (Fig. 7). **b** Outcrop picture of the bioturbated red algal-bivalve packstone facies mixed with siliciclastics in the distal slope of CB3

serpulids relative to other organisms (Fornós et al. 1997). Serpulid build-ups in low-salinity settings also grew in the Miocene of the Styrian Basin in Austria (Friebe 1994). We propose that fresh water influx in the Barranco de la Mora area lowered salinity weakening the reef and favored the development of opportunistic and pioneer organisms such as serpulids after episodes of enhanced continental runoff. *Porites* is among the coral genera that are least sensitive to salinity changes (Moberg et al. 1997; Manzello and Liman 2003), but its survivorship capacity decreases with the duration of low-salinity conditions (Manzello and Liman 2003). Elsewhere, serpulids act as pioneer organisms during repopulation of shallow-water zones under stress conditions (ten Howe and van den Hurk 1993; Climaco et al. 1997; Rosso and Sanfilippo 2005; Schlögl et al. 2008). In the more turbulent area of Polopos, the input of fresh water was probably reduced and therefore less favorable for serpulid build-ups.

After terrestrial discharges salinity normalized and *Porites* progressively recovered its role as main reef builder in the Barranco de la Mora section. CB5 represents a transitional stage from a serpulid to a *Porites*-dominated clinoform body (Fig. 3). The serpulid-red algal nodules occurring in the distal slope of CB5 (Fig. 5e) are probably fragments of serpulid build-ups, in this case with red algae, reworked by the same gravity-driven processes that exported reef-framework blocks to the distal slope. The hydrodynamic conditions of the basin became more energetic as deduced from the alternation of thin fine-grained beds and thick nodule-accumulation beds (Fig. 5f), which caused the decline of large serpulid build-ups.

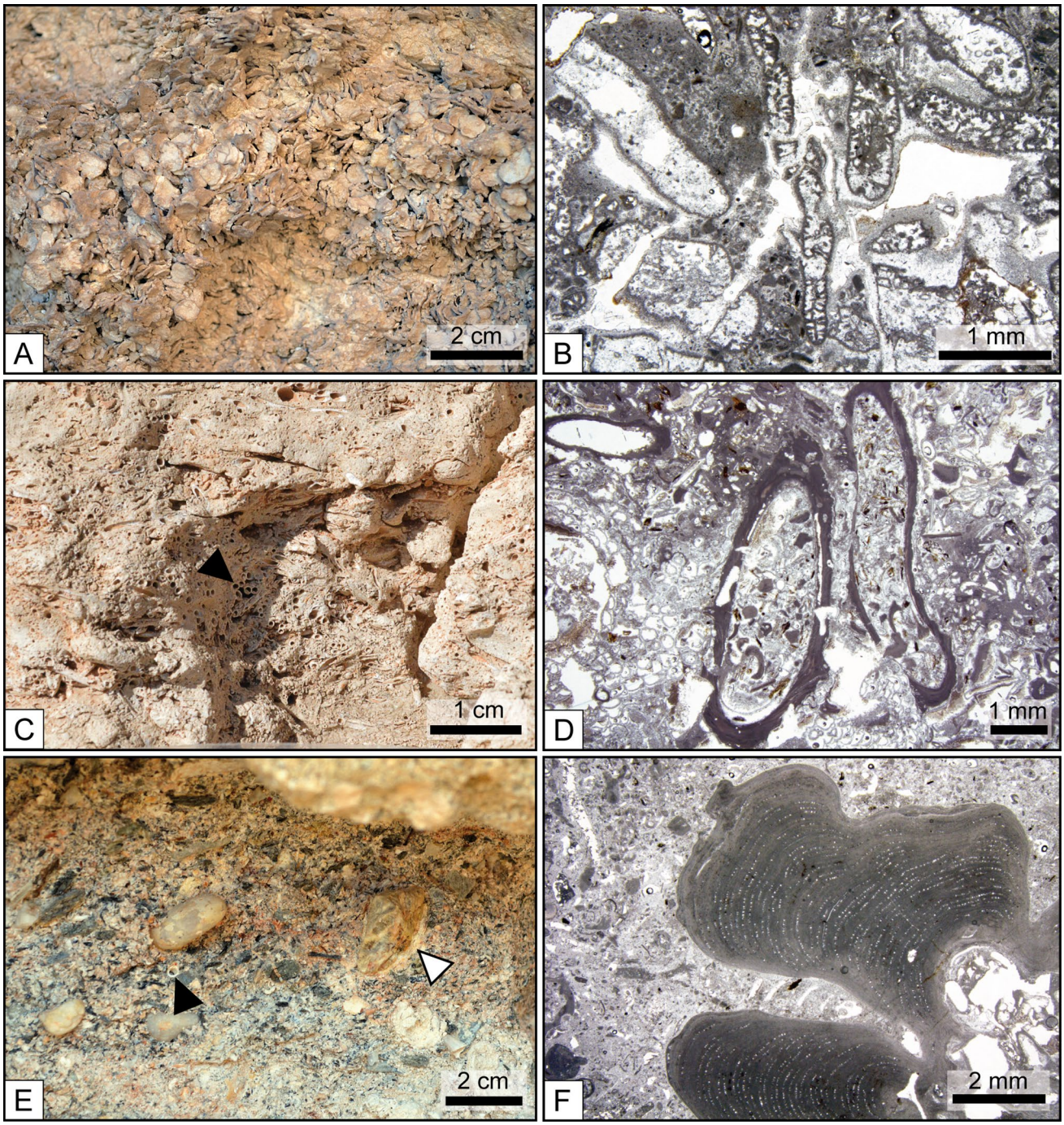

Fig. 10 Main carbonate producers of the slope facies of the Polopos carbonate platform. **a** Close-up of a talus-slope accumulation of *Halimeda* plates. **b** Photomicrograph of a *Halimeda* rudstone interval within the *Halimeda* breccia facies. **c** Outcrop picture of a serpulid patch in the siliciclastic-red algal-serpulid rudstone. **d** Photomicrograph of the siliciclastic-red algal-serpulid rudstone showing two serpulid tubes filled in with siliciclastic grains. **e** Close-up of a conglomeratic interval within the siliciclastic-red algal-serpulid rudstone with serpulid tubes (*black arrows*) and red algal crust (*white arrow*). **f** Photomicrograph of a rhodolith, red algal encrustation around a bioclasts, in the *Halimeda* breccia facies

Facies belts or facies mosaic?

Previous studies on western Mediterranean Miocene reefs described the facies distribution as belts (Pomar 1991; Pomar and Ward 1994; Dabrio et al. 1981; Franseen and Mankiewicz 1991; Riding et al. 1991; Braga and Martín 1996; Cuevas-Castell et al. 2007). Facies belts result from the combination of controlling factors such as the initial bathymetry as well as biological and sedimentary processes (Wright and Burgess 2005). The Miocene tropical carbonate platform slopes of Almería show a downslope facies zonation, i.e., facies belts, by the basinward decrease in grain size, from reef-framework blocks and breccia to fine-grained packstone (Fig. 11).

The facies distribution of the Miocene platform slope was usually assumed static in architectural and stratigraphical analyses (Braga and Martín 1996; Cuevas-Castell et al. 2007). Reolid et al. (2014), however, showed that slope facies arrays are not static, because changes in accommodation space control the relative impact of processes affecting the slope (i.e., carbonate production and gravity flows) as well as their intensity, and, in this respect, the extent and occurrence of facies belts (Fig. 11; Reolid et al. 2014). Facies patterns depended on changes in the accommodation space that control the intensity of gravity-driven processes along the slope margin and changes in the hydrography conditions of the basin (Fig. 12). The gravity-driven processes are usually triggered by collapse of the reef front (Riding et al. 1991; Reolid et al. 2014), and they may vary in occurrence and intensity along the platform edge (Fig. 12; Playton et al. 2010). These collapses also changed through time in response to sea-level fluctuations (Reolid et al. 2014). The variability associated with gravity-driven processes may result in the reduction or obliteration of some facies belts (Fig. 12). Sea-level fluctuations may also affect the facies variability, as in the case of *Halimeda*-rich facies in the Cariatiz carbonate platform that abundantly occur during relative highstands and disappear during sea-level falls and lowstands, replaced by bioclastic packstone to rudstone with common red-algae (Reolid et al. 2014).

Reolid et al. (2014) linked the dynamic behavior of slope facies belts to sea-level fluctuations. This approach, however, does not fully explain the apparently random facies distribution of the Polopos and Cariatiz carbonate platform slopes (Fig. 11). Wright and Burgess (2005), drawing on Wilkinson et al. (1999), proposed the concept of facies mosaics to characterize slopes with an arrangement of lithological elements lacking significant linear trends but showing some statistically significant relationship between element size and frequency. The processes determining the facies distribution in a mosaic could be derived for each patch of sediment (Wright and Burgess 2005), but collecting such information is difficult to impossible. Another study advocates an intermediate position between the facies belts and mosaics to explain the patchy distribution of coral framework in the northern Red Sea, and the Gulfs of Suez and Aqaba (Riegl and Piller 2000).

This work shows that the occurrence of terrestrial influx and variations of the hydrodynamic energy of the carbonate platform slopes lead to local changes of the dominant facies assemblage (Fig. 11). Such changes are independent of the accommodation space and may occur at any sea-level position (Fig. 12). Although the occurrence of continental input in the carbonate platform slopes seems to be random, the facies association related to the input is predictable (Fig. 12). We propose a banded mosaic that considers the stochastic phenomena along the slope (i.e., occurrence, of restricted areas or local terrestrial influx) but also allows predicting the depth zonation related to biological and gravity-driven processes, ultimately related to sea-level changes.

Conclusions

Miocene tropical carbonate platform slopes show classical reef-slope facies distribution but also an unexpected abundance of serpulid-rich facies, locally forming build-ups. We propose that the extensive occurrence of the serpulid-rich facies is related to recolonization of the substrate by the pioneer serpulids after hydrographical changes in the environment related to intense continental runoff. The development of large serpulid build-ups correlates to quiet hydrodynamic conditions of the slope in restricted areas of the carbonate platforms. The interplay of sea-level changes and continental supply control the facies variability laterally and along the slope, as well as through the progradation

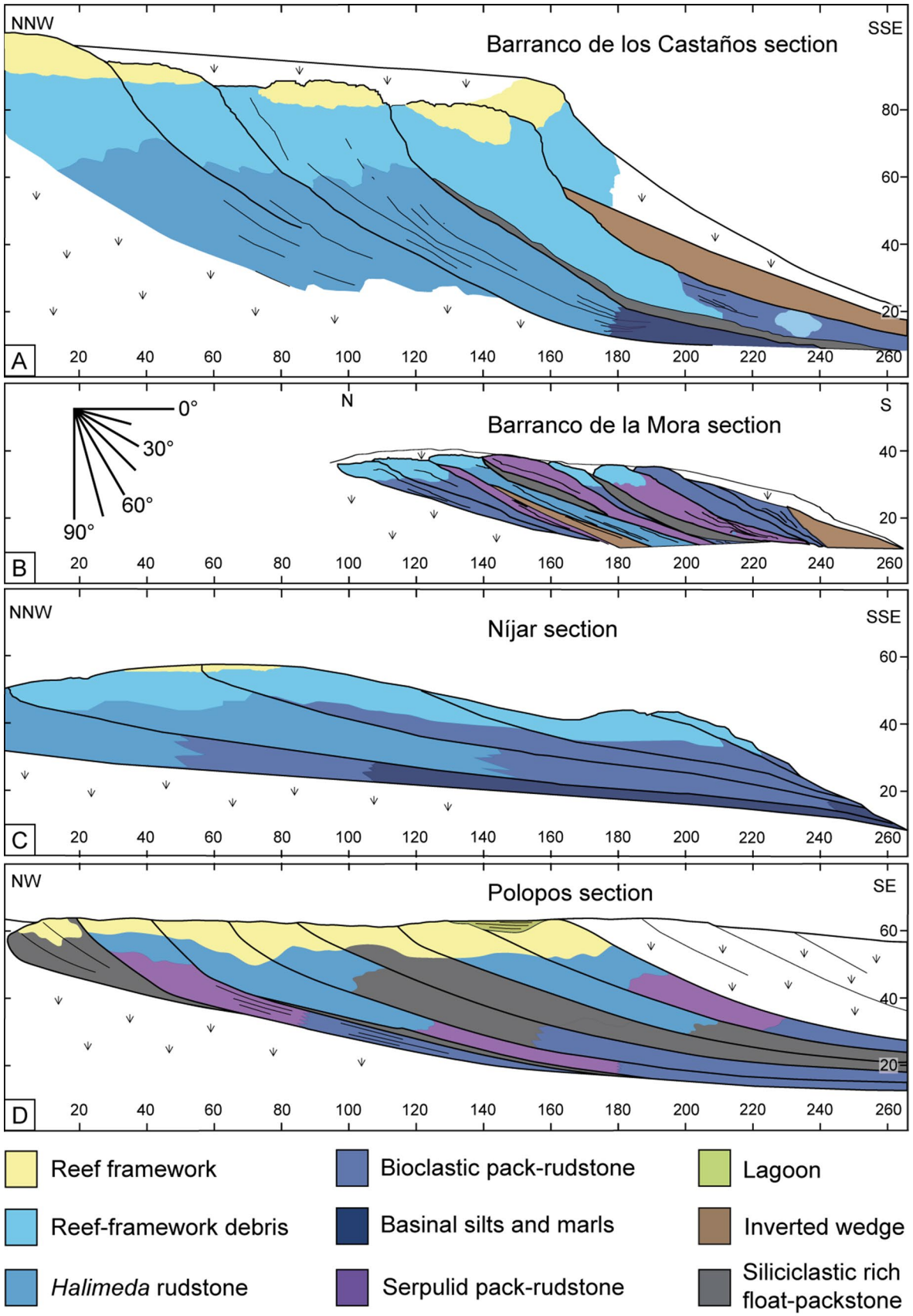
NNW
SSE
Barranco de los Castaños section
80
60
40
20
A
20 40 60 80 100 120 140 160 180 200 220 240 260
N
S
0°
30°
60°
90°
Barranco de la Mora section
40
20
B
20 40 60 80 100 120 140 160 180 200 220 240 260
NNW
SSE
Níjar section
60
40
20
C
20 40 60 80 100 120 140 160 180 200 220 240 260
NW
SE
Polopos section
60
40
20
D
20 40 60 80 100 120 140 160 180 200 220 240 260
Reef framework
Reef-framework debris
Halimeda rudstone
Bioclastic pack-rudstone
Basinal silts and marls
Serpulid pack-rudstone
Lagoon
Inverted wedge
Siliciclastic rich float-packstone

◂**Fig. 11** Comparison of Miocene tropical platform slopes from SE Spain including: **a** Barranco de los Castaños and **b** Barranco de la Mora sections in Cariatiz carbonate platform (Sorbas Basin); and the sections of the **c** Níjar carbonate platform and **d** the Polopos carbonate platform slopes (Níjar Basin)

of the carbonate platform. We suggest a new model that explains facies variability in the context of intrinsic and extrinsic factors.

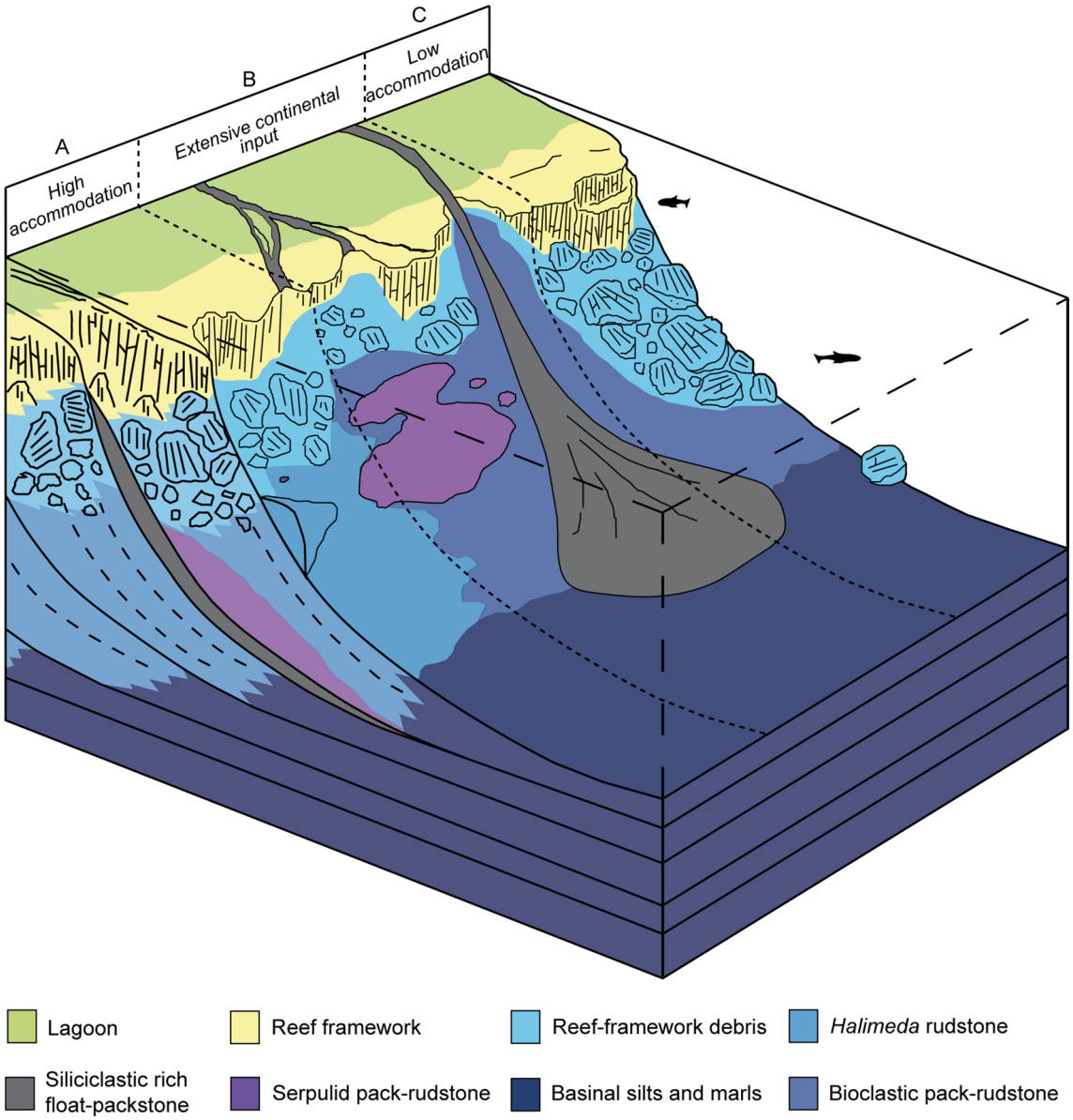

Fig. 12 Model of the facies variability in the Miocene tropical carbonate platform slopes from SE Spain (Fig. 11). *A* Slope facies distribution under conditions of increased accommodation space. Facies display a downslope decrease of grain size, from reef-framework blocks and breccia to fine-grained sediments at the distal slope, and an extensive development of *Halimeda* algae in areas with upwelling (highstand conditions; Reolid et al. 2014). *B* Facies distribution along a slope with episodic continental input. The continental influx changes the hydrographical conditions of the basin causing a poor development or absence of *Halimeda* growths. These conditions are suitable for the opportunistic serpulids that may form build-ups under quiet hydrodynamic conditions. *C* Facies distribution in slopes forming under conditions of decreased accommodation space affected by intensive rock falls and gravity flows. The extensive distribution of reef-framework debris may reduce or suppress some facies belts (Reolid et al. 2014)

Acknowledgements The authors wish to thank the German Research Foundation (Deutsche Forschungsgemeinschaft) for financial support through the Grant Be 1272/21-1 (NEOCARPS). We also wish to thank Prof. Dr. José Manuel Martín for his insightful discussions concerning the Miocene carbonate platform slopes from Almería. The authors also thank the reviewers Prof. Dr. Juan Carlos Braga and Prof. Dr. James Nebelsick for their most valuable comments. Eva Vinx is thanked for producing the thin-sections, and JR thanks Dr. Matías Reolid for his valued support in the field and the lab.

References

Adams EW, Schlager W, Wattel E (1998) Submarine slopes with an exponential curvature. Sediment Geol 117:135–141

Bosence DWJ (1973) Recent serpulid reefs, Connemara, Eire. Nature 242:40–41

Braga JC, Martín JM (1996) Geometries of reef advance in response to relative sea-level changes in a Messinian (uppermost Miocene) fringing reef (Cariatiz reef, Sorbas Basin, SE Spain). Sedimrnt Geol 107:61–81

Braga JC, Martín JM, Alcalá B (1990) Coral reefs in coarse-terrigenous sedimentary environments (Upper Tortonian, Granada Basin, southern Spain). Sediment Geol 66:135–150

Braga JC, Martín JM, Riding R (1996) Internal structure of segment reefs: *Halimeda* algal mounds in the Mediterranean Miocene. Geology 24:35–38

Braga JC, Martín JM, Quesada C (2003) Patterns and average rates of late Neogene—recent uplift of the Betic Cordillera, SE Spain. Geomorphology 50:3–26

Climaco A, Boni M, Iannace A, Zamparelli V (1997) Platform margins, microbial/serpulids bioconstructions and slope-to-basin sediments in the Upper Triassic of the "Verbicaro Unit" (Lucania and Calabria, Southern Italy). Facies 36:37–56

Cuevas-Castell JM, Betzler C, Rössler J, Hüssner H, Peinl M (2007) Integrating outcrop data and forward computer modelling to unravel the development of a Messinian carbonate platform in SE Spain (Sorbas Basin). Sedimentology 54:423–441

Dabrio CJ, Esteban M, Martín JM (1981) The coral reef of Níjar, Messinian (uppermost Miocene), Almería Province, SE Spain. J Sediment Petrol 51:521–539

Dabrio CJ, Martín JM, Megías AG (1985) The tectosedimentary evolution of Mio-Pliocene reefs in the province of Almería (SE Spain). In: Milá MD, Rosell J (eds) Sixth European regional meeting of the international association of sedimentologists. Excursion guidebook, Lleida, Spain, pp 269–305

Esteban M (1980) Significance of the Upper Miocene coral reefs of the western Mediterranean. Palaeogeogr Palaeoclimatol Palaeoecol 29:169–188

Esteban M (1996) An overview of Miocene reefs from Mediterranean areas: general trends and facies models. Models carbonate stratigraphy Miocene reef complexes of Mediterranean regions. SEPM Concepts Sedimentol Paleontol 5:3–53

Fornós JJ, Forteza V, Martínez-Taberner A (1997) Modern polychaete reefs in western Mediterranean lagoons: *Ficopomatus enigmaticus* (Fauvel) in the Albufera of Menorca, Balearic Islands. Palaeogeogr Palaeoclimatol Palaeoecol 128:175–186

Franseen EK, Goldstein RH (1996) Paleoslope, sea-level and climate controls on upper Miocene platform evolution, Las Negras area, southeastern Spain. Models for carbonate stratigraphy from Miocene reef complexes of Mediterranean regions. SEPM Concepts Sedimentol Paleontol 5:159–176

Franseen EK, Mankiewicz C (1991) Depositional sequences and correlation of middle (?) to late Miocene carbonate complexes, Las Negras and Níjar areas, southeastern Spain. Sedimentology 38:871–898

Friebe JG (1994) Serpulid-bryozoan-foraminiferal biostromes controlled by temperate climate and reduced salinity: middle Miocene of the Styrian Basin, Austria. Facies 30:51–62

Giaconia F, Booth-Rea G, Martínez-Martínez JM, Azañón JV, Pérez-Peña M, Pérez-Romero J, Villegas I (2012) Geomorphic evidence of active tectonics in the Sierra Alhamilla (eastern Betics, SE Spain). Geomorphology 145–146:90–106

Jiménez AP, Braga JC (1993) Occurrence and taphonomy of bivalves from the Níjar reef (Messinian, Late Miocene, SE Spain). Palaeogeogr Palaeoclimatol Palaeoecol 102:239–251

Mankiewicz C (1988) Occurrence and paleocologic significance of *Halimeda* in late Miocene reefs, southeastern Spain. Coral Reefs 6:271–279

Manzello D, Liman D (2003) The photosynthetic resilience of *Porites* furcata to salinity disturbance. Coral Reefs 22:537–540

Martín JM, Braga JC (1990) Arrecifes Messinienses de Almería. Tipologías de crecimiento, posición estratigráfica y relación con las evaporitas. Geogaceta 7:66–68

Martín JM, Braga JC (1994) Messinian events in the Sorbas Basin in the southeastern Spain and their implications in the recent history of the Mediterranean. Sediment Geol 90:257–268

McIlreath IA, James NP (1978) Facies models 13, carbonate slopes. Geosci Can 5:189–199

Moberg F, Nyström M, Kautsky N, Tedengren M, Jarayabhand P (1997) Effects of reduced salinity on the rates of photosynthesis and respiration in the hermatypic corals *Porites lutea* and *Pocillopora damicornis*. Mar Ecol Prog Ser 157:53–59

Pedrera A, Galindo-Zaldívar J, Marín-Lechado C, García-Tortosa FJ, Ruano P, Garrido AL, Giaconia F (2012) Recent and active faults and folds in the central-eastern internal zones of the Betic Cordillera. J Iber Geol 38:191–208

Playton TE, Janson X, Kerans C (2010) Carbonate slopes. In: James NP, Dalrymple RW (eds) Facies Models 4, GEOtext 6: Geological Association of Canada. St John's, Newfoundland, pp 449–476

Pomar L (1991) Reef geometries, erosion surfaces and high-frequency sea-level changes, upper Miocene reef complex, Mallorca, Spain. Sedimentology 38:243–269

Pomar L, Ward WC (1994) Response of late Miocene Mediterranean reef platform to high-frequency eustasy. Geology 22:131–134

Qian PY (1999) Larval settlement of polychaetes. Hydrobiologia 402:239–253

Reolid J, Betzler C, Braga JC, Martín JM, Lindhorst S, Reijmer JJG (2014) Reef slope geometries and facies distribution: controlling factors (Messinian, SE Spain). Facies 60:737–753

Riding R, Martín JM, Braga JC (1991) Coral stromatolite reef framework, Upper Miocene, Almería, Spain. Sedimentology 38:799–818

Riegl B, Piller W (2000) Reefs and coral carpets in the northern Red Sea as models for organism-environment feedback in coral communities and its reflection in growth fabrics. In: Insalaco E, Skelton PW, Palmer TJ (eds) Carbonate platform systems: components and interactions, vol 178. Geological Society, London, pp 71–88 **(special publications)**

Rosso A, Sanfilippo R (2005) Bryozoan and serpuloidean skeletobiont communities from Pleistocene of Sicily: spatial utilisation and competitive interactions. In: Fugagnoli A, Bassi D (eds) Giornata di studi paleontologici "Prof. C. Loriga Broglio", Annali dell'Università di Ferrara. Sezione di Museologia Scientifica e Naturalistica. Volume speciale 2005, Ferrara, Italy, pp 115–130

Sánchez-Almazo IM, Spiro B, Braga JC, Martín JM (2001) Constraints of stable isotope signatures on the depositional palaeoenvironments of upper Miocene reef and temperate carbonates in the Sorbas Basin, SE Spain. Palaeogeogr Palaeoclimatol Palaeoecol 175:153–172

Sánchez-Almazo IM, Braga JC, Dinarès-Turell J, Martín JM, Spiro B (2007) Palaeoceanographic controls on reef deposition: the Messinian Cariatiz reef (Sorbas Basin, Almería, SE Spain). Sedimentolology 54:637–660

Schlager W (2005) Carbonate sedimentology and sequence stratigraphy. In: North CP, Milliken KL (eds) Concepts in sedimentology and paleontology 8. SEPM, Tulsa, p 200

Schlögl J, Michalík J, Zágorsek K, Atrops F (2008) Early Tithonian serpulid-dominated cavity dwelling fauna, and the recruitment pattern of the serpulid larvae. J Paleontol 82:351–361

Sola F, Braga JC, Aguirre J (2013) Hooked and tubular coralline algae indicate seagrass beds associated to Mediterranean Messinian reefs (Poniente Basin, Almería, SE Spain). Palaeogeogr Palaeclimatol Palaeoecol 374:218–229

Ten Howe HA, van den Hurk P (1993) A review of recent and fossil serpulid 'reefs'; actuopalaeontology and the 'Upper Malm' serpulid limestones in NW Germany. Geol Mijnbouw 72:23–67

Wilkinson BH, Drummond CN, Diedrich NW, Rotman ED (1999) Poisson processes of carbonate accumulation on Paleozoic and Holocene platforms. J Sediment Res 69:338–350

Wilson JL (1975) Carbonate facies in geologic history. Springer, New York, p 471

Wright VP, Burgess PM (2005) The carbonate factory continuum, facies mosaics and microfacies: an appraisal of some of the key concepts underpinning carbonate sedimentology. Facies 51:17–23